

# Accuracy improvement of optical vector network analyzer based on single-sideband modulation

Min Xue, Shilong Pan,\* and Yongjiu Zhao

Key Laboratory of Radar Imaging and Microwave Photonics, Ministry of Education,  
Nanjing University of Aeronautics and Astronautics, Nanjing 210016, China

\*Corresponding author: pans@ieee.org

Received March 28, 2014; accepted April 29, 2014;  
posted May 15, 2014 (Doc. ID 209024); published June 11, 2014

An approach to suppress the measurement errors induced by the high-order sidebands of the optical single-sideband (OSSB) signal in the OSSB-based optical vector network analyzer (OVNA) is proposed and experimentally demonstrated. An analytical model for studying the measurement errors of the OSSB-based OVNA is established. Results show that the measurement errors introduced by the high-order sidebands can be obtained by suppressing the optical carrier in the OSSB signal. By subtracting these errors from the ordinary frequency responses measured by the OVNA, accurate frequency responses can be achieved. A proof-of-concept experiment is performed. The magnitude and phase responses of a fiber Bragg grating are measured with good coincidence by the OSSB signals with different modulation indices. © 2014 Optical Society of America

OCIS codes: (300.0300) Spectroscopy; (300.6320) Spectroscopy, high-resolution; (300.6370) Spectroscopy, microwave; (300.6380) Spectroscopy, modulation.

<http://dx.doi.org/10.1364/OL.39.003595>

The emergence of high  $Q$  optical devices with the ability to finely manipulate the optical spectrum has led to an increasing interest in developing a high-resolution optical vector network analyzer (OVNA) for measuring simultaneously magnitude and phase responses. Previously, OVNA's based on modulation phase-shifted method [1] or interferometry approach [2] were reported. In both approaches, however, the wavelength sweep is achieved by scanning the wavelength of the laser source. Due to the low wavelength accuracy and poor wavelength stability of the wavelength-swept laser source, the finest resolution of the OVNA is larger than 1 pm, which is not enough to obtain the responses of ultrahigh  $Q$  optical resonators [3,4] or ultra-narrow fiber Bragg gratings (FBGs) [5]. To improve the measurement resolution, OVNA's based on optical single-sideband (OSSB) modulation were developed [6–13]. Benefitting from mature electrical spectrum analysis technologies, the measurement resolution of the OSSB-based OVNA can reach 78 kHz in experiments [10] and several hertz in theory [6]. However, the OSSB modulator always generates considerable high-order sidebands (i.e.,  $\pm 2$ nd-,  $\pm 3$ rd-, ...,  $n$ th-order sidebands), especially when the modulator works in the large phase modulation index case, which would introduce considerable measurement errors in measuring the magnitude and phase responses [11]. Although applying unbalanced double-sideband modulation and post-signal processing, the measurement error introduced by the unwanted first-order sideband under small signal modulation can be reduced [12], there is no work in the literature to deal with the high-order-sideband induced measurement errors in the OSSB-based OVNA.

In this Letter, we propose and demonstrate a novel approach to suppress the measurement errors introduced by the high-order sidebands of the OSSB signal in the OSSB-based OVNA. Three steps are applied in the measurement. In the first step, an OSSB signal is used to obtain the frequency responses of the optical device-under-test (ODUT) with the high-order-sideband induced measurement errors. Then the optical carrier of the OSSB

signal is suppressed, and a second measurement is performed to obtain the measurement errors. Finally, the accurate frequency responses of the ODUT are achieved by subtracting the second measured results from the first results. A proof-of-concept experiment is carried out. The responses of a FBG are obtained with good coincidence by the OSSB-based OVNA with different modulation indices.

Figure 1 shows the schematic diagram of the OSSB-based OVNA with improved accuracy. An optical carrier from a laser diode (LD) is modulated by an RF signal from a tunable RF source at an OSSB modulator. The OSSB signal propagates through a tunable optical filter (TOF), which can be controlled to be an all-pass filter or a notch filter to remove the optical carrier. The output of the TOF is connected to an ODUT. In the ODUT, the magnitude and phase of the OSSB signal is changed according to the transmission response of the ODUT. Then a photodetector (PD) is incorporated to convert the OSSB signal to an RF signal. The magnitude and phase of the RF signal are extracted by a phase-magnitude detector referring to the RF signal from the RF source. By sweeping the frequency of the RF source, the frequency responses of the ODUT can be obtained.

Mathematically, the general RF modulated OSSB signal after the TOF can be written as

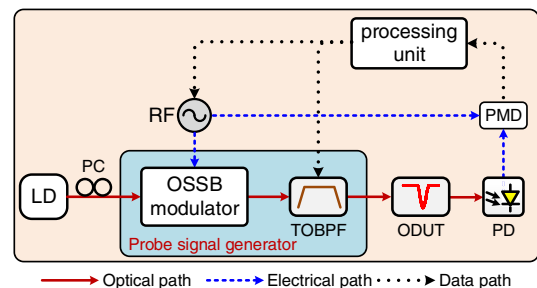


Fig. 1. Schematic of the proposed OSSB-based OVNA with improved accuracy. PC, polarization controller; RF, radio frequency; PMD, phase-magnitude detector.

$$E_{\text{in}}(\omega) = \alpha \exp(i\beta) A_0 \delta(\omega - \omega_o) + \sum_{\substack{n=-\infty \\ n \neq -1,0}}^{+\infty} A_n \cdot \delta[\omega - (\omega_o + n\omega_e)], \quad (1)$$

where  $\omega_o$  and  $\omega_e$  are the angular frequencies of the optical carrier and the RF signal, respectively,  $A_n$  is the complex amplitude of the  $n$ th-order sideband, and  $\alpha$  and  $\beta$  are the attenuation and phase shift of the optical carrier introduced by the TOF.

When this OSSB signal is transmitted through the ODUT, the magnitude and phase of the carrier and sidebands are changed according to the transmission response of the ODUT. The optical signal at the output of ODUT can be expressed by

$$E_{\text{out}}(\omega) = H(\omega) \cdot E_{\text{in}}(\omega) = \alpha \exp(i\beta) A_0 H(\omega_o) \delta(\omega - \omega_o) + \sum_{\substack{n=-\infty \\ n \neq -1,0}}^{+\infty} H(\omega_o + n\omega_e) A_n \cdot \delta[\omega - (\omega_o + n\omega_e)], \quad (2)$$

where  $H(\omega) = H_{\text{ODUT}}(\omega) \cdot H_{\text{sys}}(\omega)$ ,  $H_{\text{ODUT}}(\omega)$ , and  $H_{\text{sys}}(\omega)$  are the transmission responses of the ODUT and measurement system, respectively.

After the square-law detection in the PD, we obtain the current for the  $\omega_e$  component,

$$i_{\text{PD}}(\omega_e) = \frac{\eta}{2\pi} \alpha \exp(-i\beta) A_{+1} A_0^* H(\omega_o + \omega_e) H^*(\omega_o) + \frac{\eta}{2\pi} \sum_{\substack{n=-\infty \\ n \neq -1,0}}^{+\infty} A_{n+1} A_n^* H[\omega_o + (n+1)\omega_e] H^*(\omega_o + n\omega_e), \quad (3)$$

where  $\eta$  is the responsivity of the PD.

In the conventional measurement [6–13], the carrier is not attenuated (i.e.,  $\alpha = 1$  and  $\beta = 0$ ). Thus the photocurrent is

$$i_{\text{PD}}^R(\omega_e) = \frac{\eta}{2\pi} A_{+1} A_0^* H(\omega_o + \omega_e) H^*(\omega_o) + \frac{\eta}{2\pi} \sum_{\substack{n=-\infty \\ n \neq -1,0}}^{+\infty} A_{n+1} A_n^* H[\omega_o + (n+1)\omega_e] H^*(\omega_o + n\omega_e). \quad (4)$$

On the right-hand of Eq. (4), the first term is the actual frequency responses of the ODUT, and the second term represents the errors introduced by the beat note of the adjacent high-order sidebands. In practice, the high-order sidebands always exist especially when the phase modulation index of the modulator is large. Therefore the second term must be suppressed to ensure high accuracy of the OVNA. To do so, we can obtain purely the third term in the right-hand of Eq. (4) by letting  $\alpha \approx 0$ , i.e., the carrier of the OSSB signal is suppressed. In that case, the obtained photocurrent is given by

$$i_{\text{PD}}^E(\omega_e) = \frac{\eta}{2\pi} \sum_{\substack{n=-\infty \\ n \neq -1,0}}^{+\infty} A_{n+1} A_n^* H[\omega_o + (n+1)\omega_e] H^*(\omega_o + n\omega_e). \quad (5)$$

By subtracting the photocurrent in Eq. (5) from that in Eq. (4), the photocurrent without the errors introduced by the high-order sidebands can be obtained:

$$i(\omega_e) = \frac{\eta}{2\pi} A_{+1} A_0^* H(\omega_o + \omega_e) H^*(\omega_o). \quad (6)$$

$H_{\text{sys}}(\omega)$  can be measured by a calibration step in which the ODUT is removed and two test ports are directly connected, i.e.,  $H_{\text{ODUT}}(\omega) = 1$ . In this case, we have

$$i_{\text{sys}}(\omega_e) = \frac{\eta}{2\pi} A_{+1} A_0^* H_{\text{sys}}(\omega_o + \omega_e) H_{\text{sys}}^*(\omega_o). \quad (7)$$

According to Eqs. (6) and (7), the actual frequency responses of the ODUT without the measurement errors can be obtained, given by

$$H_{\text{ODUT}}(\omega_o + \omega_e) = \frac{i(\omega_e)}{i_{\text{sys}}(\omega_e) H_{\text{ODUT}}^*(\omega_o)}, \quad (8)$$

where  $H_{\text{ODUT}}^*(\omega_o)$  is a constant since it is the frequency response of the ODUT at a fixed wavelength.

A proof-of-concept experiment based on the setup shown in Fig. 1 is carried out. A light wave with a power of 16 dBm from a tunable laser source (Agilent N7714A) is modulated by an RF signal generated by an electrical vector network analyzer (EVNA, Agilent N5245A) at an OSSB modulator. The OSSB modulator consists of a polarization modulator (PolM) having a bandwidth of 40 GHz and a half-wave voltage of 3.5 V at 1 GHz (Versawave Inc.), a polarization controller (PC), a polarizer (Pol), and a programmable optical filter (Finisar WaveShaper 4000s) [14]. Since the WaveShaper can be controlled to suppress or keep the optical carrier, as shown in Fig. 2, the TOF is also implemented by it. A 43 GHz wideband RF power amplifier (Centellax OA4MVM3) is inserted to amplify the RF signal to a satisfactory power level. The ODUT is a FBG fabricated by TeraXion, Inc. A 50 GHz PD with a responsivity of 0.65 A/W is employed to convert the optical signal to an RF signal, which is then processed by the phase-magnitude detector in the EVNA. The optical spectra are monitored by an optical spectrum analyzer (Yokogawa AQ6370C) with a resolution of 0.02 nm.

Figure 3 shows the measured magnitude and phase responses when the modulation index is 1.68. Dividing the complex frequency response measured by the OSSB signal with optical carrier [shown in Figs. 3(a1) and 3(a2)] by that measured in the calibration process [shown in Figs. 3(b1) and 3(b2)], the magnitude and phase responses of the FBG with the high-order-sideband induced measurement errors, can be obtained as shown in Figs. 3(c1) and 3(c2). Then the magnitude and phase errors, induced by the high-order sidebands in the measurement and calibration process, can be obtained by the OSSB signal with the optical carrier suppressed, as

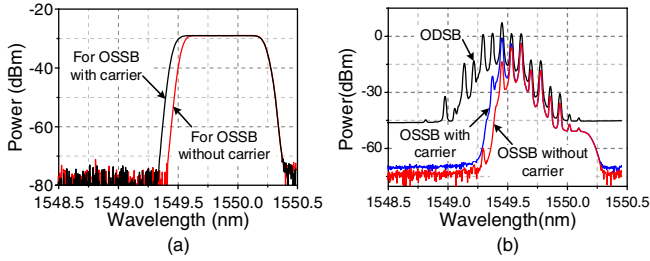


Fig. 2. (a) Filter shapes of the WaveShaper for generating the OSSB signals with and without the optical carrier. (b) Optical spectra of the optical double sideband (ODSB) signal, and the OSSB signal with and without the optical carrier.

shown in Figs. 3(d1), 3(d2), 3(e1), and 3(e2), respectively. By subtracting the errors from the responses measured in the first step, the accurate responses with smooth profiles can be obtained, as shown in Figs. 3(f1) and 3(f2).

Figure 4 shows the magnitude and phase responses of the FBG measured with and without error suppression when the modulation index is 1.68, and those measured by the proposed OSSB-based OVNA and a commercial OVNA (LUNA OVA5000) at different modulation indices. From Figs. 4(a) and 4(b), it demonstrates that the errors are greatly suppressed. As can be seen from Figs. 4(c) and 4(d), the magnitude and phase responses measured by the proposed approach are superimposed, which also agree well with those measured by LUNA OVA5000 [black solid diamond lines in Figs. 4(c) and 4(d)].

It should be noted that for different modulation indices, the dynamic ranges of the OSSB-based OVNA are different since the small electrical signal beaten by the first-order sideband, and the optical carrier might be under the noise floor especially when measuring an optical filter with deep notch. The proposed OSSB-based OVNA

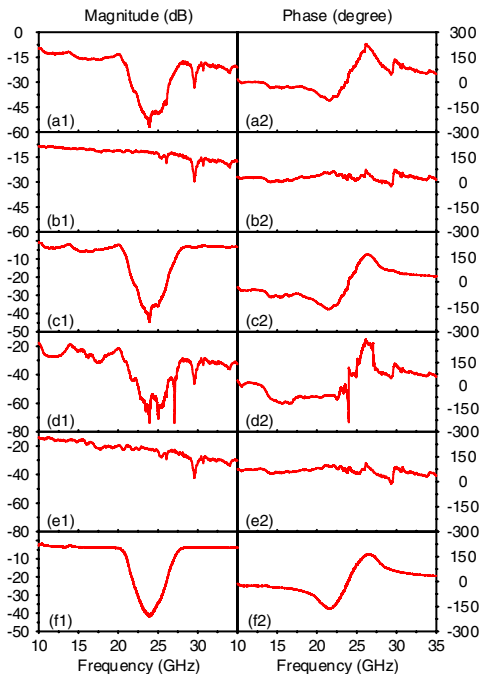


Fig. 3. Measured magnitude and phase responses when the modulation index is 1.68.

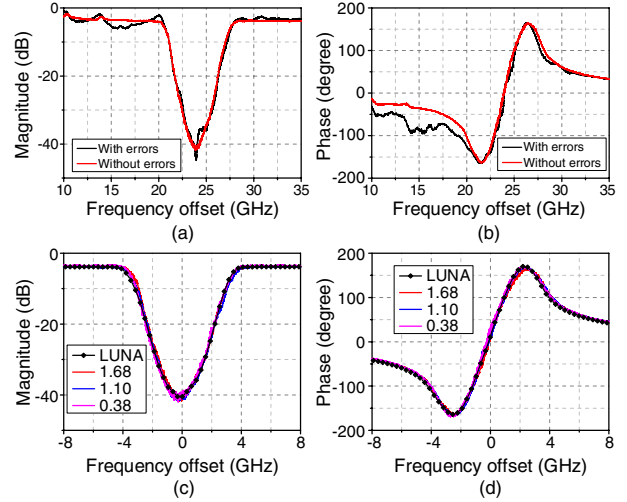


Fig. 4. (a) Magnitude and (b) phase responses of the FBG measured with and without error suppression. (c) Magnitude and (d) phase responses measured by the proposed OVNA with different modulation indices and LUNA OVA5000.

also can have a relative large dynamic range as the large modulation index can be applied.

In conclusion, an approach to suppress the errors induced by the high-order sidebands in the OSSB signal for OSSB-based OVNA was proposed and experimentally demonstrated. In the proof-of-concept experiment, the errors were greatly suppressed, even when the large modulation index was large. The proposed OSSB-based OVNA features high measurement accuracy and large dynamic range, which can be applied in fabrication, characterization and maintenance of high  $Q$  optical devices for finely manipulating the optical spectrum.

This work was supported in part by the National Basic Research Program of China (2012CB315705), the Aviation Science Foundation of China (2012ZD52052), the Jiangsu Provincial Funds for Distinguished Young Scientists (BK2012031), the Jiangsu Provincial Program for High-level Talents in Six Areas (DZXX-034), the Fundamental Research Funds for the Central Universities, Funding of Jiangsu Innovation Program for Graduate Education (CXZZ12\_0154), the Foundation of Graduate Innovation Center in Nanjing University of Aeronautics and Astronautics (kfjj20130214), and the Funding for Outstanding Doctoral Dissertation in NUAU (BCXJ13-08).

**References**

1. T. Niemi, M. Uusimaa, and H. Ludvigsen, *IEEE Photon. Technol. Lett.* **13**, 1334 (2001).
2. G. D. VanWiggeren, A. R. Motamedi, and D. M. Baney, *IEEE Photon. Technol. Lett.* **15**, 263 (2003).
3. J. Riemensberger, K. Hartinger, T. Herr, V. Brasch, R. Holzwarth, and T. J. Kippenberg, *Opt. Express* **20**, 27661 (2012).
4. I. Fescenko, J. Alnis, A. Schliesser, C. Y. Wang, T. J. Kippenberg, and T. W. Hänsch, *Opt. Express* **20**, 19185 (2012).
5. Y. Painchaud, M. Aubé, G. Brochu, and M.-J. Picard, in *Bragg Gratings, Photosensitivity, and Poling in Glass Waveguides* (Optical Society of America, 2010), paper BTuC3.

6. J. E. Román, M. Y. Frankel, and R. D. Esman, *Opt. Lett.* **23**, 939 (1998).
7. R. Hernandez, A. Loayssa, and D. Benito, *Opt. Eng.* **43**, 2418 (2004).
8. A. Loayssa, R. Hernández, D. Benito, and S. Galech, *Opt. Lett.* **29**, 638 (2004).
9. M. Sagues and A. Loayssa, *Opt. Express* **18**, 17555 (2010).
10. Z. Z. Tang, S. L. Pan, and J. P. Yao, *Opt. Express* **20**, 6555 (2012).
11. M. Xue, S. L. Pan, X. W. Gu, and Y. J. Zhao, *J. Opt. Soc. Am. B* **30**, 928 (2013).
12. M. Wang and J. P. Yao, *IEEE Photon. Technol. Lett.* **25**, 753 (2013).
13. W. Li, W. H. Sun, W. T. Wang, L. X. Wang, J. G. Liu, and N. H. Zhu, *IEEE Photon. Technol. Lett.* **26**, 866 (2014).
14. Z. Z. Tang and S. L. Pan, in *2013 IEEE Topical Meeting on Microwave Photonics* (IEEE, 2013), paper W4-27.